journal

J. Am. Ceram. Soc., 98 [3] 774–780 (2015)
DOI: 10.1111/jace.13380

Influence of Particle Size on Nonisothermal Crystallization in a Lithium Disilicate Glass

Leyliane E. Marques,[‡] Alberth M. C. Costa,[‡] Murilo C. Crovace,[§] Ana C. M. Rodrigues,[§] and Aluisio A. Cabral[‡,¶,†]

[‡]Postgraduate Program in Materials Engineering, Federal Institute of Maranhão, IFMA, São Luis, Maranhão 65030-001, Brazil

[§]Vitreous Materials Laboratory, LaMaV, Department of Materials Engineering, DEMa, Federal University of São Carlos, UFSCar, São Carlos, São Paulo 13565-905, Brazil

[¶]Physics Department, Federal Institute of Maranhão, IFMA, São Luis, Maranhão 65030-001, Brazil

In this study, lithium disilicate (LS_2) glass samples with different particle sizes ranging from less than 105 to 850 μm were prepared. These specimens were inserted in a Pt-Rh DSC crucible and heated to 850°C at different rates (ϕ = 0.5–30 K/min) to identify their crystallization peaks. The activation energies for the overall crystallization (E) and the Avrami coefficient (n) were evaluated using different nonisothermal models. Specifically, n was evaluated using the Augis–Benett model and the Ozawa method, and E was evaluated using the Kissinger and Ligero methods. As expected, the coarse particles mainly crystallized in the volume, while surface crystallization was predominant in the samples with particle sizes of less than 350 μm. This result was confirmed through SEM analysis of the double stage heat-treated samples. In contrast with previous studies, our results demonstrated that the activation energy decreased as the particle size increased. In addition, no clear correlation between the peak intensity (δT_p) and the particle size was observed.

I. Introduction

Glass-ceramics are materials that are obtained under controlled glass crystallization conditions. The microstructure and properties of the glass-ceramics depend on the heat treatments employed. To tailor this microstructure, it is important to understand the temperature dependencies of the crystal nucleation [$I(T)$] and crystal growth [$U(T)$] rates. In addition, glass crystallization can occur simultaneously and competitively from the surface and the bulk sample. Nevertheless, depending on several conditions, such as the time of heat treatment, temperature, atmosphere, humidity, etc., one of these crystallization mechanisms can dominate over the others. The Avrami coefficient, n, is useful for identifying predominant crystallization mechanisms[1] because a value of n close to 3 suggests bulk or three-dimensional crystal growth, and a value close to 1 is consistent with surface growth. However, the variations of some characteristic parameters of the crystallization peak, such as the temperature reciprocal ($1/T_p$) and intensity (δT_p), with the heating rate can be used for this purpose. Depending on the overlapping degree of the $I(T)$ and $U(T)$ curves, these parameters are proportional to the number of nuclei that are formed during the nucleation regime, as demonstrated by Ref. [2].

It is well known that the total density of nuclei formed in a glass (N_t) can be expressed as:

$$N_t = N_q + N_s + N_h + N_i \quad (1)$$

where N_q is the concentration of quenched-in nuclei or pre-existing nuclei; N_s corresponds to the number of active surface nuclei, N_h is the bulk nuclei formed during the DSC run, and N_i is the bulk nuclei formed during the nucleation heat treatment.

Considering as-quenched glasses, $N_i = 0$. In addition, if all the samples are prepared from the same batch, N_q must be constant. Under these conditions, any change in the shape of the DSC peak may result from the contribution of N_h and N_s, where N_h is proportional to the reciprocal of the heating rate.

The Avrami coefficient can be calculated through the Augis–Bennet equation, which is given by the following expression:

$$n = \frac{2.5}{\Delta T_p}\frac{RT_p^2}{E} \quad (2)$$

where E is the activation energy for the overall crystallization, which includes crystal nucleation and growth, R the gas constant and ΔT_p and T_p are the corresponding half-width and temperature of the DTA crystallization peak, respectively.

Marotta & Buri.[3] were pioneers for nonisothermal devitrification investigations of LS_2 glass. Based on DTA runs at several heating rates (1°C/min–50°C/min) that were conducted on powdered samples (63–88 μm) and using nonisothermal models, these authors obtained, an average crystallization activation energy of 60 kJ/mol, which agreed with previous reports in the literature that used isothermal conditions.

In the same year, Matusita & Sakka[4] investigated nonisothermal crystallization of LS_2 glass with different particle sizes over a large range of heating rates (ϕ = 0.5–80 K/min). These authors concluded that the corresponding activation energy decreases as the particle size increases. In addition, these authors found that the dominant crystallization mechanism for each particle size was dependent on the heating rate because the contributions of surface crystallization were more evident when the heating rate increased.

Two years later, Marotta and co-workers[5] conducted two sets of DTA runs using as-quenched and nucleated specimens at 475°C for 14 h. For these sets, powdered (coarse and fine particles) and bulk samples were used. They observed that due to the high nuclei density that was formed, the crystallization peak of the nucleated specimens were narrower and shifted to lower temperatures than those of the as-quenched samples. By comparing bulk and powdered non-nucleated and nucleated samples, these authors also demonstrated that the crystallization peak of the bulk specimens became narrower

L. Pinckney—contributing editor

Manuscript No. 35579. Received September 5, 2014; approved November 14, 2014.
[†]Author to whom correspondence should be addressed. e-mail: aluisio_cab@yahoo.com.br

and shifted toward a higher temperature than those of the powdered glasses, where the bulk nucleated ones presented major volume crystallization. In addition, the finest particles exhibited predominant surface crystallization. Nevertheless, these researchers proposed that surface and bulk crystallization had the same activation energy.

By using DTA and SEM techniques to investigate the devitrification behavior in a $NaPO_3$ glass, Branda *et al.*[6] concluded that the correct interpretation of the experimental results provided by the DTA methods should be confirmed by complementary techniques to clarify the crystallization mechanisms and the activation energy of crystal growth. These authors obtained different n and E values for the same $NaPO_3$ glass depending on the crystal morphology.

Beginning with Eq. (2) and assuming that the activation energy is independent of the particle size, Ray and Day[7] conducted DTA runs on several lithium disilicate (LS_2) glasses that were prepared under different conditions. This study was conducted to promote surface or volume crystallization by adjusting the particle size, by exposing the glass particles to moist air at 100% relative humidity, or by doping them with low concentrations of platinum. The experiments were performed at a fixed heating rate from room temperature until complete crystallization and nearly the same mass. The dry and wet LS_2 glasses showed decreasing tendencies of (δT_p) and $\frac{T_p^2}{\Delta T_p}$ with increasing particle size. In addition, an increasing tendency of (δT_p) and $\frac{T_p^2}{\Delta T_p}$ with increasing particle size was observed for the LS_2 glass that was doped with 0.005 wt% Pt. Therefore, these authors concluded that the changes in the (δT_p) or $\frac{T_p^2}{\Delta T_p}$ ratio of the DTA crystallization peak on the particle size could predict whether the glass mainly crystallizes on the surface or through bulk crystallization, i.e., a decreasing or $\frac{T_p^2}{\Delta T_p}$ with increasing particle size indicated predominant surface crystallization, while increasing values indicated bulk (internal) crystallization.

As a continuing study, Ray *et al.*[8] investigated the changes of these parameters with particle size for several glass compositions, including some tellurite glasses (bad glass formers). Using DTA runs and examining their microstructures by Scanning Electron Microscopy (SEM), these authors confirmed that the glasses that were mainly bulk crystallized were characterized by increases in (δT_p) and $\frac{T_p^2}{\Delta T_p}$ with increasing particle diameter, while decreasing (δT_p) indicated that surface crystallization was predominant.

Furthermore, Ray *et al.*[9] investigated the crystallization kinetics of as-quenched LS_2 glass particles of different sizes by heating the particles in DTA at 15°C/min from room temperature until the completion of crystallization. These authors observed a logarithmic decreasing dependence of δT_p with particle size, which was attributed to the increasing surface to volume ratio as the particle size decreased. In addition, these authors observed that the T_p changes with the particle size. Nevertheless, they did not calculate the E and n values for each glass particle size.

Recently, Karamanov *et al.*[10] investigated the influence of particle size on the crystallization mechanisms in a glass with a composition of $54SiO_2{\cdot}2Al_2O_3{\cdot}21CaO{\cdot}21MgO{\cdot}2Na_2O$ (% mol), which is characterized by a surface crystallization of ~60 wt% diopside ($CaO{\cdot}MgO{\cdot}2SiO_2$) and by the formation of 8–10 vol% porosity during crystallization. Nonisothermal DTA analysis showed that the activation energy for crystallization decreased as the particle size increased. In addition, the Avrami coefficient increased as the particle sizes decreased, reaching 2.5 for the smallest particle sizes. This tendency was confirmed by the SEM images of the isothermal heat-treated samples, which highlighted that the crystals, even for fine particles, were three dimensional during the initial crystal growth stage. In addition, dendritic growth was observed during the larger particle growth phase.

As one can see from this extensive review, there are two main points of view about the change in activation energy according to particle size, which can be divided into two groups:

1. Marota *et al.*[5] and Ray *et al.*[7–9]: First, it must be emphasized that Marota *et al.*[5] obtained different values of activation energy for overall crystallization for bulk and powdered LS_2 samples, where $E_{(bulk)} < E_{(powder)}$. However, they assumed that the number of nuclei formed during heating was negligible, i.e., $N_h = 0$, which means that crystallization occurred only through growth from a fixed number of nuclei. Thus, they concluded that this decrease was not real, and suggested that surface and bulk crystallization had the same activation energy. Taking into account the findings of Marota *et al.*,[5] Ray *et al.*[7–9] assumed that the activation energy does not change with particle size.
2. Matusita & Sakka[4] and Karamanov *et al.*[10] found that the values of crystallization activation energy obtained for LS_2 and $54SiO_2{\cdot}2Al_2O_3{\cdot}21CaO{\cdot}21MgO{\cdot}2Na_2O$ (% mol) glasses, respectively, decreased as the particle size increased because of the change in the corresponding crystallization mechanism.

As demonstrated above, controversial results are presented in the literature regarding the changes in the activation energy with particle sizes. These controversial results occur even when only LS_2 model glass is considered. Therefore, using the (δT_p) dependence with the particle diameter to infer the predominant crystallization mechanism is not clear. In addition, a complementary technique must be used to correctly interpret the experimental results obtained using DTA/DSC methods. Therefore, this study aimed to investigate the possible changes of the E and n values in LS_2 glass that was prepared using different particle sizes [PD1 (<105 μm), PD2 (105–355 μm), PD3 (350–425 μm), PD4 (425–600 μm) and PD5 (600–850 μm)]. To test the reproducibility of the results, the DSC runs were conducted under the same conditions (using the same crucibles, atmosphere and masses). In addition, SEM images were obtained from the isothermally heat-treated PD1 and PD5 samples to observe the crystal morphology and the predominant crystallization mechanism (i.e., surface or volume).

II. Theory

The formal theory of phase transformation and the nonisothermal models proposed to evaluate the main crystallization kinetic parameters have been discussed extensively in several papers (e.g., Henderson[11] and Yinnon and Uhlmann[12]). Thus, only a brief summary of the main equations used in this study is provided below.

This theory was independently derived by Johnson–Mehl–Avrami–Yerofyeyev–Kolmogorov (JMAYK) and provides a correct interpretation of the thermal analysis experiments. The well-known JMAYK equation is given as follows:

$$x(t) = 1 - \exp(Kt)^n \tag{3}$$

where $x(t)$ is the crystallized fraction as a function of time, n is the dimensionless Avrami coefficient, which varies between 0.5 and 4, can be related to the mechanism of crystallization and provides qualitative information regarding the nature of the nucleation process and crystal growth, and K is the reaction rate constant. Over a narrow temperature range, $K(T)$ can be written according to the Arrhenius equation as follows:

$$K = K_0 \exp\left(-\frac{E}{RT}\right) \tag{4}$$

where K_o is a frequency factor, E is the activation energy for the overall transformation (crystallization), and R is the gas constant.

The following equations are obtained by combining Eqs. (3) and (4):

$$\ln[-\ln(1-x)] = n\ln(t) + n\ln(K) \tag{5}$$

and

$$\ln K = \ln K_o - E/RT \tag{6}$$

From the $\ln[-\ln(1-x)]$ versus $\ln(t)$ plot, a straight line is obtained for which the slope and intercept are numerically equal to n and K, respectively. The crystallization activation energy can be estimated from known ln K values at some temperatures.

According to the Ozawa model,[13] the heating rate (ϕ) is proportional to the changing temperature with time [i.e.,$\phi = \left(\frac{T-T_o}{t}\right)$]. Therefore, Eq. (3) can be rewritten as:

$$x = 1 - \exp\left[-K\left(\frac{T-T_0}{\phi}\right)\right]^n \tag{7}$$

By applying the logarithm to both terms in Eq. (7), the following equation is obtained:

$$\ln[\ln(1-x) = n\ln[K(T-T_0)] - n\ln(\phi) \tag{8}$$

When assuming a fixed temperature and deriving Eq. (8) in terms of ϕ, the following equation is obtained:

$$\frac{\mathrm{d}\ln(-\ln(1-\mathrm{x}))}{\mathrm{d}\ln\phi}|_{\mathrm{T}} = -n \tag{9}$$

where n is the Avrami coefficient. Therefore, n can be estimated from the slope of the straight line provided by a plot of ln [−ln (1 − x)] versus ln(ϕ).

The n parameter can also be evaluated from the Augis–Bennett[14] Equation, which is given by the aforementioned Eq. (2). Nevertheless, this model can only be used if the activation energy is known.

By taking the logarithm of the crystallization rate ($\mathrm{d}x/\mathrm{d}t$), Ligero *et al.*[15] obtained an expression that established a linear relationship between the logarithm of $\mathrm{d}x/\mathrm{d}t$ and the inverse absolute temperature, which is given as

$$\ln\left(\frac{\mathrm{d}x}{\mathrm{d}t}\right) = \ln[K_0 f(x)] - \frac{E}{RT} \tag{10}$$

According to this expression, a linear relationship exists between $\ln(\mathrm{d}x/\mathrm{d}t)$ and the inverse of the absolute temperature because $f(x)$ is constant over a given interval of x values. In addition, by assuming two given values of the crystallized fraction (x_1 and x_2) in which $\ln[K_o.f(x)]$ is constant, the Avrami exponent can be evaluated using the following equation:

$$n = \ln\left[\frac{\ln(1-x_2)}{\ln(1-x_1)}\right]\left\{\ln\left[\frac{(1-x_2)\ln(1-x_2)}{(1-x_1)\ln(1-x_1)}\right]\right\}^{-1} \tag{11}$$

The Kissinger method[16–18] is another kinetic approach that is used to analyze DSC/DTA data, which is given by the expression given below:

$$\ln\left(\frac{T_p^2}{\phi}\right) = \frac{E}{R}\frac{1}{T_p} + cte \tag{12}$$

Here, the activation energy can be estimated from the slope of the straight lines that results from plotting $\ln(T_p^2/\phi)$ versus $1/T_p$.

In this study, we applied the models proposed by Ligero, Ozawa, Augis–Bennett and Kissinger to study the kinetics of LS_2 glass crystallization as a function of particle size.

III. Experimental Procedures

The reagents and the batch synthesis conditions, such as the crucible, melting and remelting temperatures, and the corresponding times used to prepare the model lithium disilicate glass ($Li_2O{\cdot}2SiO_2$–LS_2) were described by Everton and Cabral.[19]

Furthermore, the samples were milled and sieved into different particle size fractions with grain sizes of PD1 (<105 μm), PD2 (105–355 μm), PD3 (350–425 μm), PD4 (425–600 μm) and PD5 (600–850 μm). Samples of each particle size with the same mass (20.5 mg) were heated at 0.5, 1, 3, 5, 8, 10, 15, 20, 25 and 30 K/min in a NETZSCH STA 449C thermal analyzer (NETZSCH-Geratebau GmbH, Selb, Germany) to determine the crystallization peak. The measurements were conducted under an argon atmosphere (20 cm^3/min) and the equipment was temperature calibrated periodically during the measurements using $RbNO_3$, $KClO_4$, CsCl, K_2CrO_4, and $BaCO_3$ standards.

The PD1 and PD5 glass powders were heat treated in a hot stage microscope (MISURA HSM ODHT, Expert System Solutions, Modena, Italy). The samples were poured into a piece of a 4 mm alumina rod over a 10 mm × 8 mm × 1 mm aluminum plaque. Then, the samples were heat treated in the HSM furnace with the following schedule: (i) room temperature to 380°C at 80°C/min ($T_g \approx 454$°C), with a dwelling time of 10 min to reduces the temperature gradient inside the furnace chamber; (ii) 380°C to 480°C at 80°C/min to form new nuclei (this temperature was maintained for 20 min); (iii) 480°C to 620°C at 80°C/min, where they were kept for 20 min to develop nuclei with detectable sizes under the scanning electron microscope; and (iv) a rapid temperature change from 620°C to 24°C.

After the heat treatments, the HSM samples were embedded in an epoxy resin (EpoThin™; Buehler, Lake Bluff, IL) under vacuum and were cured for 24 h at room temperature. Next, the samples were carefully ground with silicon carbide grit 1200 paper and polished with CeO_2 solution before ultrasonic cleaning. Finally, the samples were sputter coated with gold for 30 s (Q150R ES; Quorum, Lewes, East Sussex, UK) and analyzed using Scanning Electron Microscopy (FEG XL-30; Philips, Eindhoven, The Netherlands).

IV. Results

(1) Crystallization Peaks

Because the DSC curves of all the powder samples presented the same tendencies, Fig. 1 depicts a portion of the DSC runs that were obtained for the PD1 and PD5 samples. When considering a fixed particle size, the crystallization peaks shifted to higher temperatures as the heating rate increased and the corresponding height became more intense. Furthermore, by comparing the DSC curves that were registered for the different glass particles, it was observed that the crystallization peak of the coarse particles becomes narrower and shifts toward a high temperature relative to those of the finest powders, corresponding with the findings of Marotta and Buri.[5]

By integrating the curves depicted in Fig. 1, the evolution of the crystallized volume fraction (%) was determined in terms of the temperature at each heating rate for PD1 and PD5, as shown in Fig. 2.

In Fig. 2, the complete crystallization of each glass particle was shifted to higher temperatures as the heating rates increased. This behavior occurred because less time was spent during heating and more residual glass remained until complete crystallization of the LS_2 samples was achieved. For all heating rates, Fig. 2 shows that the temperature of the crystallization peak of PD5 is greater than the temperature

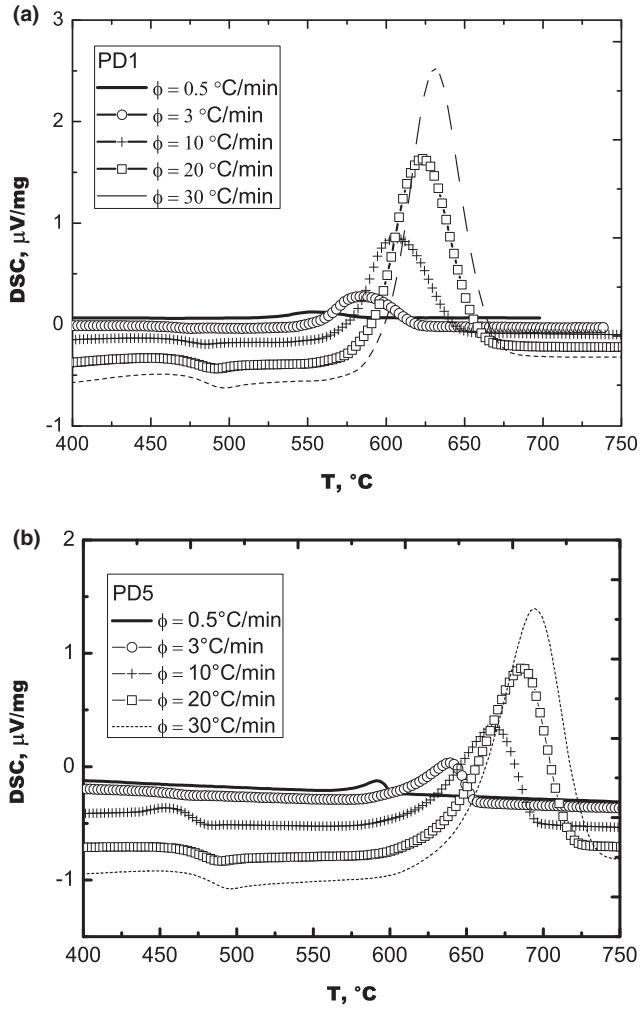

Fig. 1. Part of the DSC runs obtained from the nonisothermal experiments for (a) PD1 and (b) PD5. Some heating rates are indicated in the plot.

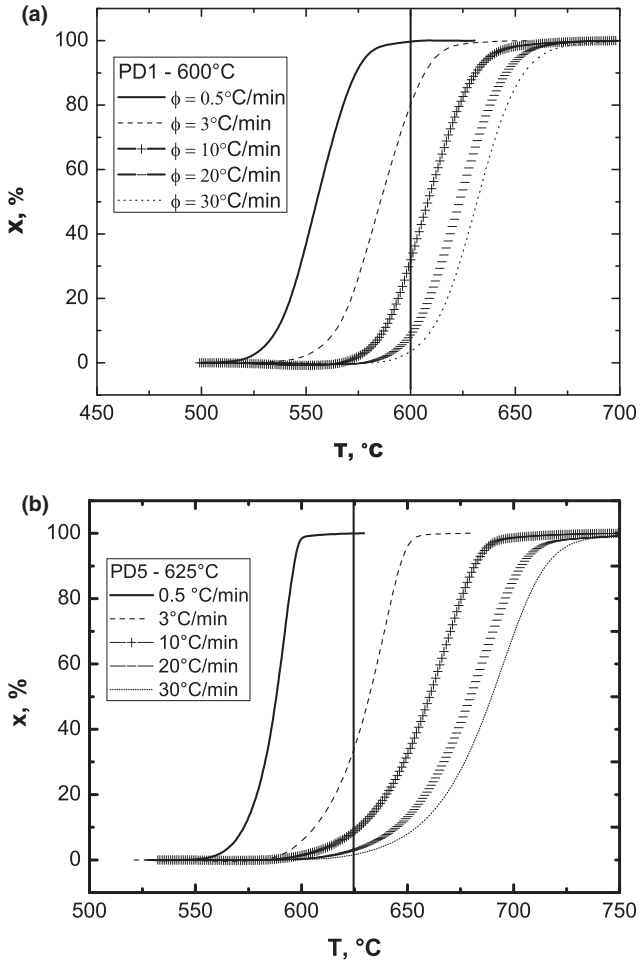

Fig. 2. The crystallized volume fraction (x) as a function of temperature obtained for (a) PD1 and (b) PD5 glasses. The corresponding vertical lines indicate the fixed temperatures that were used to estimate x for each heating rate [600°C (PD1) and 625°C (PD5)]. These values were used to calculate n with the Ozawa model.

obtained for PD1. This behavior is related to the high specific surface area of PD1, which accelerates the formation of nuclei on the surface.

(2) Kissinger Model

Based on the peak crystallization temperatures (Fig. 1), the graphs of $\ln\left(\frac{T_p^2}{\phi}\right)$ versus $\frac{1}{T_p}$ were created for each glass particle (Fig. 3). The values of E were calculated from the slopes of these graphs and are presented in Table I.

(3) Ligero Model

Because the plots of $\ln(dx/dt)$ against the inverse absolute temperatures ($1/T$) that were obtained for each glass particle were similar, Fig. 4 shows the Ligero plot for the PD3 sample using the same crystallized volume fraction (x) and different heating rates. In this plot, a linear relationship is observed ($r^2 = 0.99$) from $x = 0.10$–0.40. The E values that were calculated by the Ligero model are presented in Table I.

(4) Ozawa Model

Based on Fig. 2 and by fixing the temperatures at 600°C (PD1 and PD2), 625°C (PD3 and PD5) and 635°C (PD4), the plots of $\ln[-\ln(1-x)]$ versus $\ln(\phi)$ were obtained for each glass particle size (Fig. 5). The values of n that were calculated from the slopes of the straight lines are presented in the second column of Table II.

(5) Augis-Bennett Model

By considering the activation energies that were calculated through the Kissinger model (Table I) and the values of T_p and ΔT_p that were obtained from the DSC curves for each glass particle size under different heating rates, the Avrami coefficient was calculated from Eq. (2). These results are presented in Table II.

According to Table II and independent of the chosen model, the Avrami coefficient increased as the particle size increased.

V. Discussion

In agreement with previous studies,[2,9] the results illustrated in Fig. 1 show that $1/T_p$ increases as the heating rate decreases for all glass particles. Nevertheless, in contrast with these same authors,[2,9] (δT_p) increased as the heating rate increased.

To better understand this opposite behavior, one must keep in mind that, as demonstrated by Weinberg[20] and Kelton,[21] (δT_p) is proportional to the nuclei number only under certain conditions, such as: (i) a constant crystal growth rate, i.e. when the crystallization peak position does not depend on the number of nuclei and the glass composition does not change during crystallization[22]; (ii) the crystallization occurs from a fixed number of nuclei. In this case, the nucleation is completed prior to the crystal growth event. As one can see in Cabral *et al.*,[22] the composition of a LS_2 stoichiometric glass does not change during the crystallization path. As in

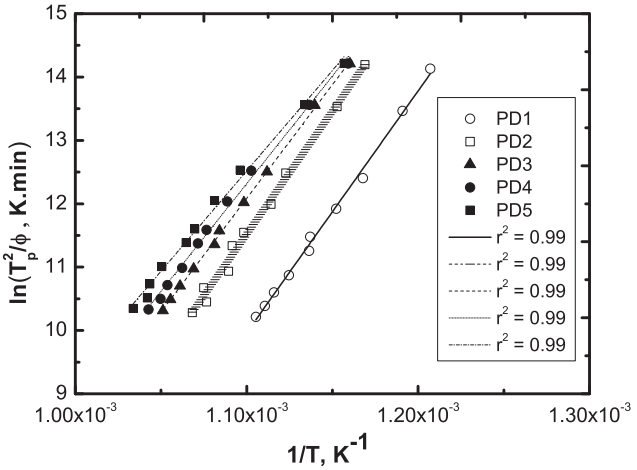

Fig. 3. $\ln(T_p^2/\phi$ as a function of the $1/T$ values that were obtained for the powder LS_2 samples. The corresponding correlation factors (r^2) are presented for each particle size.

Table I. Activation Energy Values That Were Estimated for the Different LS_2 Glass Particles Using the Kissinger and Ligero Methods

	E, kJ/mol	
Samples	Kissinger	Ligero
PD1	317 ± 6.5	321 ± 1.7
PD2	322 ± 10	307 ± 6.3
PD3	298 ± 2.7	291 ± 2.2
PD4	282 ± 6.1	266 ± 5.2
PD5	263 ± 6.9	243 ± 3.9

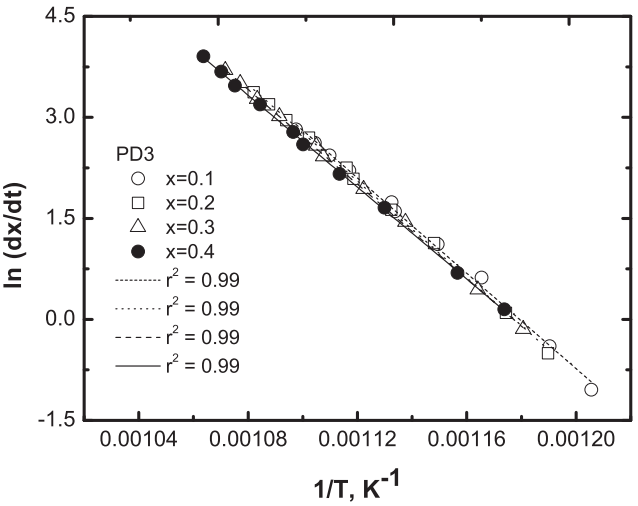

Fig. 4. Plot of ln (dx/dt) versus $1/T$ for the same crystallized fraction (x) using the Ligero method. The corresponding correlation factors (r^2) are presented for some selected volume fractions.

the present paper the powder samples were heated from room temperature until crystallization was complete, their crystallization did not occur from a fixed number of nuclei.

Therefore, this result confirms that $1/T_p$ can more accurately predict the changing of nuclei density as a function of time, since the higher the crystal number the faster is the overall crystallization kinetics and, hence, the release of the heat of crystallization can be detected at a lower temperature. Furthermore, (δT_p) should not be universally employed as a useful parameter to estimate the evolution of the

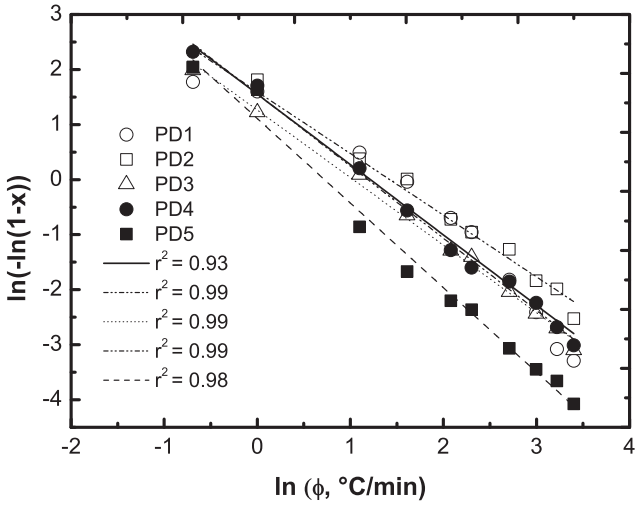

Fig. 5. Plots of ln[−ln(1−x)] versus ln ϕ obtained for each particle size. The temperatures were fixed at 600°C (PD1 and PD2), 625°C (PD3 and PD5) and 635°C (PD4). The corresponding correlation factors (r^2) are presented for each particle size.

Table II. The *n* Values Calculated for Different Particle Sizes Following the Ozawa and Augis–Bennett Models

Samples	Ozawa	Augis–Bennett
PD1	1.22 ± 0.11	1.1 ± 0.07
PD2	1.47 ± 0.09	0.97 ± 0.06
PD3	1.22 ± 0.02	1.22 ± 0.25
PD4	1.31 ± 0.03	1.78 ± 0.48
PD5	1.53 ± 0.06	2.05 ± 0.68

number of nuclei, since it is highly sensitive to the sample thermal history. By comparing the DSC curves of the different glass particles that were used in this study for all heating rates, it was observed that the DSC peak of PD5 became narrower and shifted toward higher temperatures compared with the DSC peak of PD1. This finding was previously demonstrated by Marotta and Buri,[5] and occurred because PD1 had the highest specific surface area, which accelerated the formation of nuclei on the surface.

According to Table I, the activation energies estimated by the Kissinger and Ligero methods reasonably agree. In addition, these values follow the same tendencies (i.e., E decreases as the glass particle increases).

From Table II, the values of n that were calculated here using the Ozawa and Augis-Bennet models are in reasonable agreement and indicate that the crystallization mechanism of LS_2 glass changes with the particle size [i.e., crystallization mainly occurred on the surfaces of the finest glass particles (PD1) and on a fixed number of nuclei on the largest particles (PD5)].

The observed changes in E and the variations of n reinforced the hypothesis that the crystallization mechanisms of each glass particle changed because E and n depend on T_p according to the Kissinger and Ozawa equation. This result is attributed to the increasing surface to volume ratio as the glass particle size decreases because the contributions of the surface crystallization become more significant.[9]

To confirm changes in the crystallization mechanism, Fig. 6 shows the SEM images of the PD1 and PD5 heat-treated samples. As shown in Fig. 6(a), the particles of the PD1 powder are fully crystalline and the crystallization fronts that result from the surface have encountered in the center of the particles. Furthermore, pores were formed due to the difference in the density between the LS_2 crystalline phase and the parent glass. No single crystals were observed,

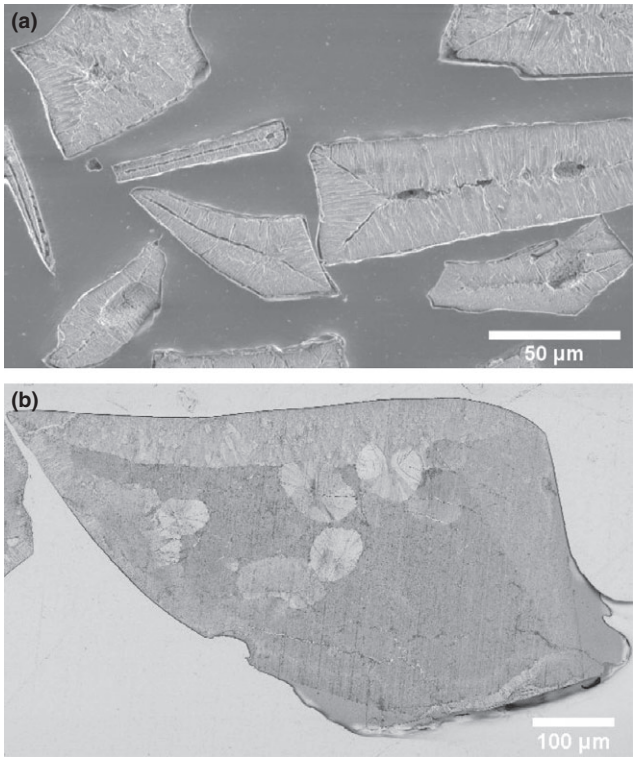

Fig. 6. SEM images of the PD1 (a) and PD5 (b) powders that were heat-treated in the hot stage microscope.

which confirmed that the PD1 mainly crystallizes from the surface. In contrast, the PD5 particles [Fig. 6(b)] showed crystalline layers and some ellipsoidal crystals, which indicated that their crystallization was predominantly internal. During cooling, some cracks were formed due to the different thermal expansion coefficients of the crystalline and the residual glass phases.

Finally, one question remains unanswered: Can the dependency of (δT_p) on the particle size be used to estimate the predominant crystallization mechanism?

Figures 7 and 8 present the plots of (δT_p) and $(T_p^2)/\Delta T$ as a function of the glass particle size, respectively. As these plots presented similar trends for all heating rates, only the results obtained for 15°C/min and 30°C/min are shown.

As shown in Figs. 7 and 8, the plots of δT_p and $(T_p^2)/\Delta T$ against the glass particle size exhibit identical behavior for

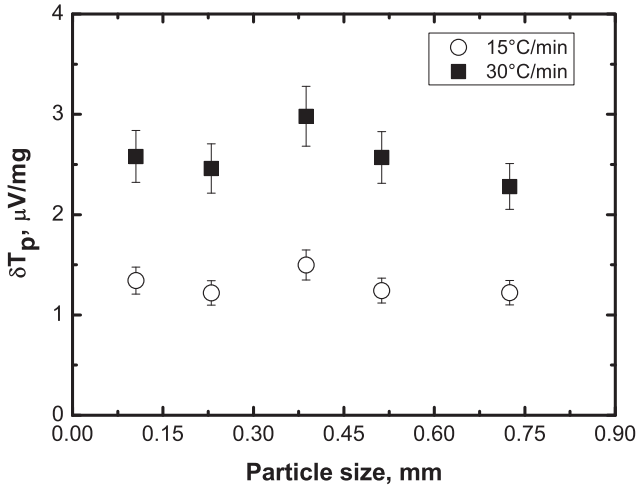

Fig. 7. Changing of δT_p as a function of the glass particle size using two different heating rates.

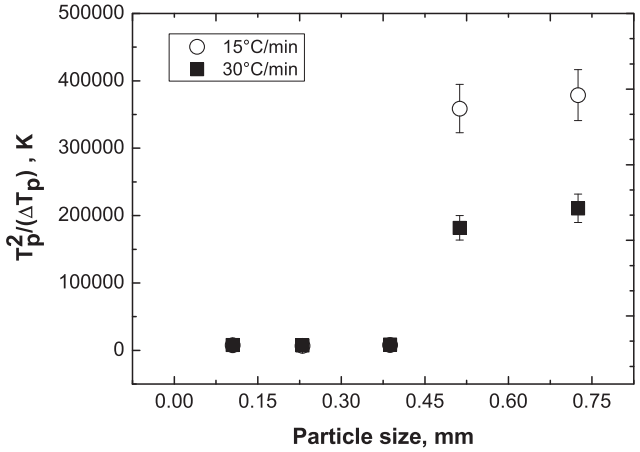

Fig. 8. Variation of $(T_p^2)/\Delta T_p$ as a function of glass particle size using two different heating rates.

all heating rates (as expected).[8] Nevertheless, in contrast with the findings of Ray *et al.*,[8] neither curve shows a clear correlation between the plots of δT_p versus particle size and $(T_p^2)/\Delta T$ versus particle size, independent of the chosen heating rate. This finding resulted from the changing activation energy with the glass particle size. Therefore, the dependency of δT_p with the glass particle size was not sufficient for predicting the predominant crystallization mechanism of a given glass.

VI. Conclusions

In this study, DSC and SEM techniques were used together for the first time to investigate the crystallization mechanisms of LS_2 glass powders with different particle sizes. Independent of the chosen model used, our results indicated that E and n depend on the particle size and that the crystallization activation energy generally decreases as the particle size increases. The variations of E and n reinforce the hypothesis that the crystallization mechanisms of each glass particle change. This phenomenon occurred because the surface to volume ratio increased as the glass particle size decreased because the contributions of the surface crystallization became more significant.[9]

The SEM observations indicated that the PD1 glass samples were mainly crystallized from the surface, while the crystallization of the PD5 glass particles was predominantly internal.

Finally, no clear correlation between the (δT_p) and $(T_p^2)/\Delta T$ parameters and the glass particle size were observed. Therefore, we conclude that these parameters were not suitable for predicting the predominant crystallization mechanisms of a given glass.

Acknowledgments

The authors are indebted to the Brazilian research funding agencies of CNPq (National Council for Scientific and Technological Development), Process # 2013/304542, CAPES (Federal Agency for the Support and Improvement of Higher Education), Process # 2008/2365, FAPEMA (Maranhão Foundation for Scientific Research and Development), Process # 2013/00628, and FAPESP-CEPID process # 2013/07793-6.

References

[1]I. S. Gutzow, O. V. Mazurin, J. W. P. Schmelzer, S. V. Todorova, B. B. Petroff, and A. I. Priven, *Glasses and the Glass Transition*. John Wiley & Sons, Weinheim, Germany, 2011.

[2]A. M. Rodrigues, A. M. C. Costa, and A. A. Cabral, "Effect of Simultaneous Nucleation and Crystal Growth on DSC Crystallization Peaks of Glasses," *J. Am. Ceram. Soc.*, **95** [9] 2885–90 (2012).

[3]A. Marotta and A. Buri, "Kinetics of Devitrification and Differential Thermal Analysis," *Thermochim. Acta*, **25**, 155–60 (1978).

[4]K. Matusita and S. Sakka, "Kinetic-Study on Crystallization of Glass by Differential Thermal-Analysis: Criterion on Application of Kissinger Plot," *J. Non-Cryst. Sol.*, **38–9**, 741–6 (1980).

[5]A. Marotta, A. Buri, and F. Branda, "Surface and Bulk Crystallization in Non-Isothermal Devitrification of Glasses," *Thermochim. Acta*, **40**, 397–403 (1980).

[6]F. Branda, A. Buri, A. Marotta, G. Mascolo, "The Non-Isothermal Devitrificação of Sodium Metaphosphate Glass," *Thermochim. Acta*, **98**, 363–6 (1986).

[7]C. S. Ray and D. E. Day, "Identifying Internal and Surface Crystallization by Differential Thermal Analysis for the Glass-to-Crystal Transformations," *Thermochim. Acta*, **280–281**, 163–74 (1996).

[8]C. S. Ray, Q. Yang, W. Huang, and D. E. Day, "Surface and Internal Crystallization in Glasses as Determined by Differential Thermal Analysis," *J. Am. Ceram. Soc*., **79** [12] 3155–260 (1996).

[9]C. S. Ray, D. E. Day, W. Huang, K. L. Narayan, T. S. Cull, and K. F. Kelton, "Non-Isothermal Calorimetric Studies of the Crystallization of Lithium Disilicate Glass," *J. Non-Cryst. Solids*, **204**, 1–12 (1996).

[10]A. Karamanov, I. Avramovi, L. Arrizza, R. Pascova, and I. Gutzow, "Variation of Avrami Parameter During non-Isothermal Surface Crystallization of Glass Powders with Different Sizes," *J. Non-Cryst. Solids*, **358**, 1486–90 (2012).

[11]D. W. Henderson, "Thermal Analysis of Non-Isothermal Crystallization Kinetics in Glass Forming Liquids," *J. Non-Cryst. Solids*, **30**, 301–15 (1979).

[12]H. Yinnon and D. R. Uhlmann, "Applications of Thermoanalytical Techniques to the Study of Crystallization Kinetics in Glass-Forming Liquids, Part **I:** Theory," *J. Non-Cryst. Solids*, **54**, 253–75 (1983).

[13]T. Ozawa, "Kinetics of Non-Isothermal Crystallization," *Polymer*, **12**, 150–8 (1971).

[14]J. A. Augis and J. E. Bennett, "Calculation of the Avrami Parameters for Heterogeneous Solid-State Reactions Using a Modification of the Kissinger Method," *J. Therm. Anal*., **13**, 283–92 (1978).

[15]R. A. Ligero, J. Vázques, P. Villares, and R. Jiménez-Garay, "A Study of the Crystallization Kinetics of Some Cu–As–Te Glasses," *J. Mater. Sci*., **26**, 211–5 (1991).

[16]H. E. Kissinger, "Variation of Peak Temperature with Heating Rate in Differential Thermal Analysis," *J. Res. Nat. Bur. Stnd*, **57**, 217–21 (1956).

[17]H. E. Kissinger, "Reaction Kinetics in Differential Thermal Analysis," *Anal. Chem*., **29**, 1702–6 (1957).

[18]R. L. Blaine and H. E. Kissinger, "Homer Kissinger and the Kissinger Equation," *Thermochim. Acta*, **540**, 1–6 (2012).

[19]L. S. Everton and A. A. Cabral, "Determining the Kinetic Parameters for Isothermal Crystallization in a Lithium Disilicate (LS_2) Glass by OM and DSC," *J. Am. Ceram. Soc*., **97** [1] 157–62 (2014).

[20]M. C. Weinberg, "Interpretation of DTA Experiments Used for Crystal Nucleation Rate Determinations," *J. Am. Ceram. Soc*., **74** [8] 1905–9 (1991).

[21]K. F. Kelton, "Estimation of the Nucleation Rate by Differential Scanning Calorimetry," *J. Am. Ceram. Soc*., **75** [9] 2449–52 (1992).

[22]A. A. Cabral, V. M. Fokin, and E. D. Zanotto, "On the Determination of Nucleation Rates in Glasses by Nonisothermal Methods," *J. Am. Ceram. Soc*., **93** [9] 2438–40 (2010). □